

# THE NIP MECHANICS OF NANO-IMPRESSION LITHOGRAPHY IN ROLL-TO-ROLL PROCESS MACHINES

By

**Yao Ren and J. K. Good**  
**Oklahoma State University**  
**USA**

## ABSTRACT

Nano-Impression Lithography (NIL) has been demonstrated to produce nano features on webs that have value to society. Such demonstrations have largely been the result of NIL processes that involve the discrete stamping of a mold with nano-impressions into a thermoplastic web or a web coated with resin that is cured during the imprint process. To scale NIL to large area products which can be produced economically requires the imprinting to occur on roll-to-roll (R2R) process machines. Nip mechanics is a topic which has been explored in relation to drive nips and winding nips in R2R machines. Nip rollers will be needed to imprint webs at production speeds to ensure mold filling on an imprint roller. The objective of this paper is to demonstrate while the nip roller is required that it can also induce imperfections in the imprinted nano-features. Successful imprinting will require nip loads sufficient to fill the imprint mold and then addressing the nip mechanics which can induce shear and slip that could destroy the nano-features. The objective is to demonstrate through the study of nip mechanics that this shear and slip can be inhibited through the selection of nip materials and tension control of the web entering and exiting the nipped imprint roller.

## NOMENCLATURE

$a$	half nip contact width [mm]
$e$	base of the natural logarithm
$E_o$	Young's modulus of the rubber cover [MPa]
$F$	nip load [N/cm]
$h$	coating thickness [nm]
$h_f$	feature thickness [nm]
$IRHD$	International Rubber Hardness Degree
$NIT$	nip induced tension [MPa]
$P_{avg}$	average pressure in the nip contact zone [KPa]
$R$	nominal radius of the imprint roller [cm]

$R_{backup}$	radius of the backup roller [cm]
$R_{imprint}$	radius of the imprint roller in simulation [cm]
$t$	time duration the average pressure is applied [ms]
$t_r$	rubber cover thickness of the backup roller [cm]
$T, T_{web}$	tension in the web [MPa]
$T_{entry}$	upstream tension in the web as the web enters nip contact zone [MPa]
$T_{exit}$	downstream tension in the web as the web exits the NIT unit [MPa]
$T_{out}$	tension in the web after the web exits the nip contact zone [MPa]
$V$	process velocity or web velocity [m/s]
$W$	feature width of molds [mm]
$x$	coordinate, origin centers in the contact zone, range $[-a, a]$ [mm]
$\eta$	viscosity of resin or thermoplastic in T-NIL [Pa·s]
$\mu$	coefficient of friction
$\nu_r$	Poisson's ratio of the rubber cover of the backup roller
$\omega_{imprint}$	angular velocity of the imprint roller [rad/s]
$\omega_{coater}$	angular velocity of the coater roller [rad/s]

## INTRODUCTION

NIL has shown the potential to develop products that are useful to society [1-3]. The nano-impressions that are imprinted on these products have the capacity to modify light that is either transmitted through or reflected from the product. There are two processes that can be used for NIL. These include the thermal NIL (T-NIL) and the ultraviolet cure (UV-NIL) processes. Both of these processes began as discrete processes where a stamp with an imprint mold was developed. In the T-NIL process a stamp would be pressed at elevated temperature into a thermoplastic which would then be imprinted. In the UV-NIL process the stamp would be pressed into uncured polymer resin that had been coated on a surface, perhaps a plastic film. UV light is then directed through the film to cure the resin prior to retraction of the stamp. The stamp pressures for the T-NIL process are relatively high when compared to that required for UV-NIL processes. In either process the stamp pressure must be sufficient to fill the mold. Typically the stamp pressure must be much higher for thermoplastics than for uncured resin based on viscosity. For society to see benefit of NIL products it is necessary to scale from these discrete stamping processes up to continuous R2R processes. The imprint mold now becomes integral with the surface of a driven roller (known as the imprint roller). A backup roller, commonly covered with an elastomer, would be used to provide the nip pressure required to fill the mold in either a T-NIL or UV-NIL process. Rolling contact often generates contact shear stresses that can induce slippage between webs and rollers [4] and between web layers in winding rolls [5,6].

A schematic diagram of a UV-NIL process is shown in Figure 1. At the left a web enters a coating process where a coating of UV curable resin is applied to the web. The coated web enters a loaded nip roll pair composed of an imprint roller and a backup roller. The mold on the imprint roller must be filled. The mold filling depends on the resin viscosity ( $\eta$ ), the time duration ( $t$ ) in the nip contact zone of width ( $2a$ ) and the average pressure in the nip contact zone ( $P_{avg}$ ). Depending on viscosity and nip roller pair design the mold filling could limit process speed ( $V$ ). NIL is possible in R2R process machines without a nip roller, in that case the pressure of contact ( $P_{avg} = T_{web}/R$ ) is controlled by web tension ( $T_{web}$ ) and the nominal radius of the imprint roller ( $R$ ). The pressure of contact without a backup roller is typically quite low which would necessitate

low process velocity. The time required to fill simple molds can be predicted using a fluid squeeze film damping equation [1, 7]:

$$t = \frac{\eta W^2}{2P_{avg}} \left( \frac{1}{h_f^2} - \frac{1}{h^2} \right) \quad \{1\}$$

where  $h$  is the coating thickness,  $h_f$  is the minimum mold feature thickness and  $W$  is a mold feature length. When no backup roller is present, the pressure of contact ( $P_{avg}$ ) is present for the period of time the coated web is in contact with the imprint roller (arc of contact divided by the web velocity). When a loaded backup roller is present, the pressure of contact is applied for a time period governed by the nip contact width ( $2a$ ) divided by the web velocity ( $V$ ).

The assumption will be made that a loaded nip backup roller will be required to achieve process speeds that will allow the scaling of NIL processes. It should be noted that Equation {1} is applicable to T-NIL processes as well where ( $\eta$ ) is now the viscosity of the thermoplastic. In T-NIL processes the thermoplastic web may be pre-heated with additional heat provided at the imprint roller to decrease the viscosity and the pressures required to fill the mold.

## THE NIP MECHANICS OF NIL

Contact mechanics will govern the pressures of contact and any potential slippage that could result in damage of the imprinted nano-features. A base line Case 1 shown in Figure 2 will be studied followed by sub-studies to show the impact of select variables. The web in these simulations is polyester, it is 51  $\mu\text{m}$  thick and assumed to be isotropic with a Young's modulus of 4.8 GPa and Poisson's ratio 0.36. The rubber cover on the backup roller is 12.7 mm thick ( $t_r$ ). The rubber will be modeled as an isotropic elastic material whose properties can completely defined with Young's modulus and Poisson's ratio. Rubber is often characterized by hardness in units of International Rubber Hardness Degree (equivalent to Shore A). Good [8] proved through testing of many synthetic rubber types and samples that the following equation could be used to convert rubber hardness to Young's modulus of elasticity:

$$E_o = 145.7e^{0.0564IRHD} \text{ (MPa)} \quad \{2\}$$

Good also proved through additional tests that for the same group of test samples that Poisson's ratio for rubber ( $\nu_r$ ) was 0.458. Good's tests were performed in accordance with ASTM D575 [9].

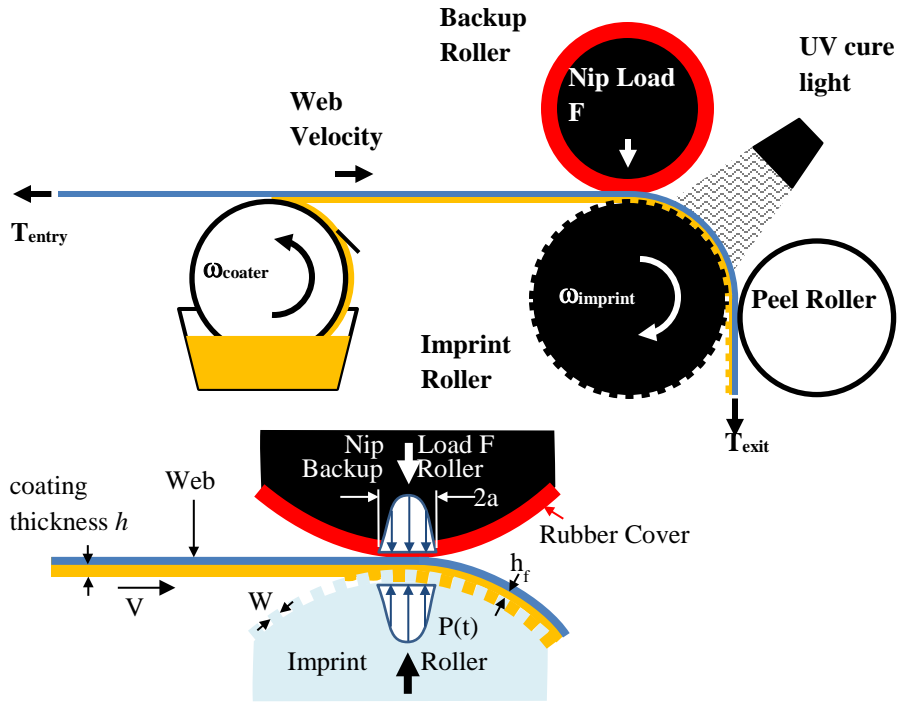


Figure 1 – A Coated Web Entering a UV-NIL Process

This method of characterization has been proven to be accurate for large deformations where other characterizations (Mooney-Rivlin, etc.) have difficulty converging in dynamic simulation. Good [8] also proved through tests that equations derived by Johnson [10] were useful in determining nip pressure distribution:

$$P(x) = \frac{(1-\nu_r)^2}{1-2\nu_r} \frac{E_o}{1-\nu_r^2} \frac{a}{2Rt_r} \left(1 - \frac{x^2}{a^2}\right) \quad \{3\}$$

where the nip contact zone width is  $2a$ ,  $R$  is the equivalent radius in contact defined as  $1/(1/R_{backup} + 1/R_{imprint})$  and  $x$  is a coordinate whose origin is centered in the contact zone and ranges from  $-a$  to  $+a$ . From this Equation {3} an average pressure of contact can be determined that is useful in Equation {1}:

$$P_{avg} = \frac{(1-\nu_r)^2}{1-2\nu_r} \frac{E_o}{1-\nu_r^2} \frac{a}{3Rt_r} \quad \{4\}$$

Johnson [10] also produced an equation that would allow the prediction of the half width of contact:

$$a = \sqrt[3]{\frac{3FRt_r(1-2\nu_r)(1-\nu_r^2)}{2E_o(1-\nu_r)^2}} \quad \{5\}$$

where  $F$  is the nip load in units of load per unit width. This allows the calculation of the time duration the average pressure is applied:

$$t = \frac{2a}{V} = \frac{2a}{R_{\text{imprint}} \omega_{\text{imprint}}} \quad \{6\}$$

In the dynamic simulations the upstream tension will be held constant at 3.45 MPa in all cases. Coulomb's Law for friction will be used. The friction coefficient between the web and the rubber cover was assumed to be 0.4. The friction coefficient between the web and metal roller surfaces was assumed to be 0.3. Implicit dynamic simulations will be conducted using Abaqus/Standard<sup>1</sup>. In the simulations the imprint, peel and the interior of the backup roller are modelled as rigid analytical surfaces. The web is modelled with plane strain elements with 3 elements through the depth such that bending stresses in the web were well modelled. Note the imprint roller is constrained against all translation and is allowed to rotate about the central out-of-plane axis, the peel roller is constrained similarly. The backup roller is constrained similarly to the imprint and peel rollers with the exception of allowing the center of the roller to move horizontally, facilitating the input of a nip load that could be varied. At the beginning of the simulation the angular velocity of the imprint roller was held at zero while the nip load and the upstream and downstream tensions were ramped to their steady state values. Finally the angular velocity of the nip roller increased from zero to 4 rad/s. After all stresses achieved steady state the output database was examined. Contact pressures within the nip contact zone, variation of the mean MD stress in the web through the contact zone and then through the exit wrap of the imprint roller and slippage of the coated web were subjects of interest.

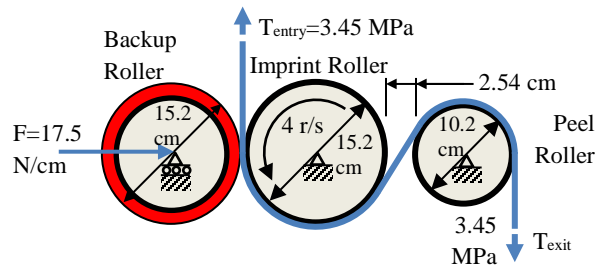


Figure 2 – Base Line Case 1

<sup>1</sup> Dassault Systems, Abaqus Simulia, Rising Sun Mills, 166 Valley St., Providence, RI 02909-2499

## DISCUSSION OF RESULTS

Results from the dynamic simulation of Case 1 are shown in Figure 3. In Figure 3(a) the contact pressure distribution in the nip contact zone is presented. Note the agreement between Equation {3} and the simulation results are good. Oscillations in contact pressure are observed in the simulation results at the entry of the nip contact zone. The entry web was defined in a vertical attitude such that it would be in surface contact with the imprint roller with no nip load present. After the nip load is input to the backup roller and rotation of the imprint roller has commenced, the simulations show that in fact the entering web first contacts the deformed rubber cover on the backup roller prior to entry of the nip contact zone. It is the complexity of this entrance condition that is responsible for these oscillations, note the oscillatory behavior is not present as the web exits the nip contact zone in Figure 3(a) where the web now is tracking the surface of the imprint roller. A web entry geometry that prevents contact with the backup roller cover prior to entry of the nip contact zone would be preferable. Nevertheless the half width of contact ( $a$ ) from Equation {5} of 4.91 mm is very comparable to that of the simulation (5.03 mm). It is evident the parabolic distribution in pressure given by Equation {3} differs from the simulation result. The average pressure in the contact zone from the simulation is 172 KPa. The average pressure given by Equation {4} is 178 KPa, very comparable to the estimated value. For purposes of design the use of Equations {4} and {5} in conjunction with Equation {1} can be used to estimate filling of the mold. The time duration the average pressure exists from the simulation is 33 mS, very comparable to the 32 mS per Equation {6}. This time duration must be larger than the time needed to fill the mold. The MD membrane stresses are shown in Figure 3(b). The nip induces slippage that causes the membrane stress to increase from the entry tension level of 3.45 MPa up to about 3.78 MPa. This increase in MD stress has been called the Nip-Induced-Tension when winding rolls of web with an impinging nip roller [5,6]. The slippage between the web and the imprint roller is shown spatially in Figure 4. The increase in MD stress is coincident with slippage shown in Figure 3(c) in the entry and exit regions of the contact zone. The increased MD stress does become a concern near the exit of the web from the imprint roller. The increased MD stress must decrease to the MD stress associated with web tension to achieve equilibrium, this can occur only through slippage for thin webs. The zone of slippage is very evident in Figure 3(d). The features that have been imprinted should be cured by the time the web exits the imprint roller such that they can release without damage. With increased process velocities to support the scaling of nano-manufacturing of these surfaces the time duration for curing on the imprint roller may be limited. It is essential the contact shear stresses be minimized to prevent damage to the imprinted features. For Case 1 this slippage is occurring over a 20.1 mm distance prior to exit of the imprint roller with the potential to damage or destroy the features that have been imprinted.

Also note there is an increase in MD membrane stress as the web transits the peel roller in Figure 3(b). This is due to the bending of the web being restricted by frictional forces as it conforms to the roller. It is evident that this smaller increase in MD membrane stress is also decaying through slippage back to the stress level associated with web tension at the peel roller exit. This slippage is not a concern as the imprinted features face outward and do not contact the peel roller. This does not mean that slippage due to bending effects can always be ignored as in some cases the imprinted features may be in contact with rollers in the process line.

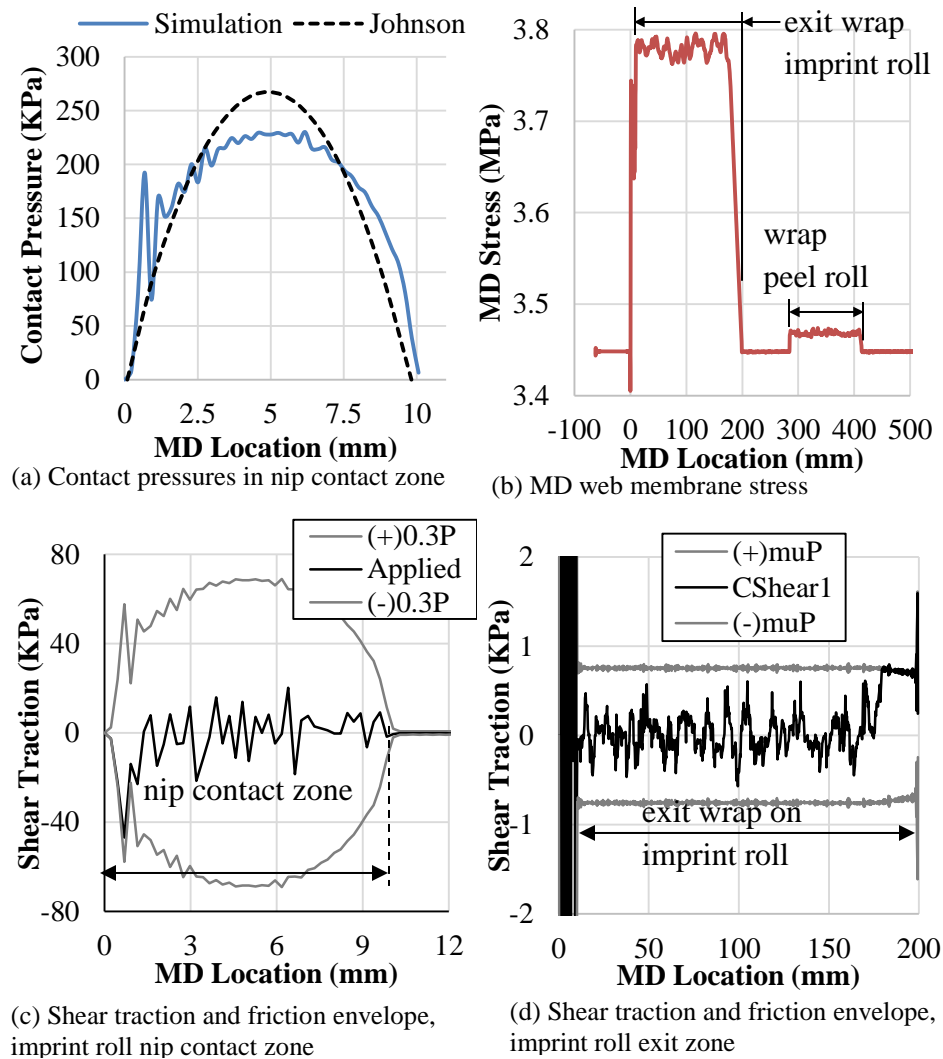


Figure 3 – Simulation Results for Case 1

After the behavior was witnessed for the base Case 1 curiosity arose with respect to the effect of variables such as nip load, web exit tension and elastomer selection for the backup roller. There are many other variables that could be studied such as web thickness and material properties, rubber thickness, backup and imprint roller radius and multiple layer covers for the backup roller. A set of simulation cases was devised as shown in Table 1. Cases 2 and 3 are similar to Case 1 and explore the effect of nip load. Cases 4 and 5 are similar to Case 1 but explore the effect of different rubber cover hardness for the backup roller. Cases 6 and 7 are similar to Case 1 but explore the effect of low Poisson ratio elastomers that are achievable with open and closed cell foams. Finally Cases 8 and 9 are similar to Case 4 and explore if the slippage at the exit of the imprint roller can be limited through control of the downstream tension ( $T_{exit}$ ).

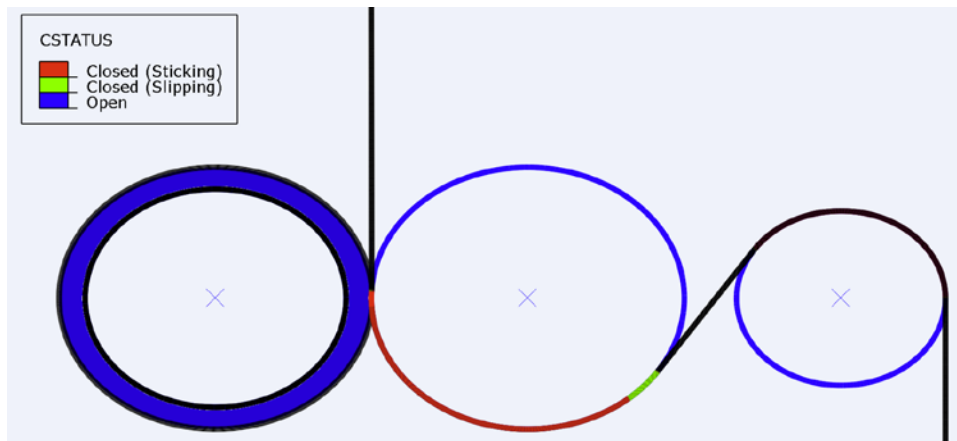


Figure 4 – Contact status showing regions of stick and slip for Case 1.

Case	Nip Load (N/cm)	$T_{exit}$ (MPa)	$v_r$	$E_r$ (IRHD)	$E_r$ (MPa)
1	17.5	3.45	0.458	50	2.42
2	1.75	3.45	0.458	50	2.42
3	8.75	3.45	0.458	50	2.42
4	17.5	3.45	0.458	30	0.785
5	17.5	3.45	0.458	40	1.38
6	17.5	3.45	0.2	50	2.42
7	17.5	3.45	0.3	50	2.42
8	17.5	4.0	0.458	30	0.785
9	17.5	4.5	0.458	30	0.785

Table 1 – Simulation Cases

The results of these simulations are shown numerically in Table 2 in terms of the average pressure in the nip contact zone, the half width of contact and the slip of the web at the exit of the imprint roller. Also shown is the ability of Equations {4} and {5} to predict the average pressure in the nip contact zone and the half width of contact. The equations performed well with the exception of Cases 6 and 7 where lower Poisson's ratio were studied. Based upon all results presented in Table 2 while Equations {4} and {5} are not exact they agree well enough to be useful for projections of mold filling in conjunction with Equations {6} and {1}. Note the slip results reported in Table 2 have signs. A positive slip is defined as slippage of the web forward with respect to the imprint roller surface towards the exit. A negative slip is defined as the web slipping upstream with respect to the imprint roller surface.



Case	Pavg (KPa)		a (mm)		Slip (mm)
	Simulation	Expr. (4)	Simulation	Expr. (5)	Simulation
1	172	178	5.03	4.91	-20.1
2	49.4	38	1.60	2.28	-11.9
3	117	112	3.66	3.89	-16.2
4	112	122	7.78	7.14	-24.7
5	138	147	6.29	5.92	-21.3
6	161	112	5.37	7.78	0.23
7	165	120	5.26	7.29	0
8	112	122	7.78	7.14	9.60
9	112	122	7.78	7.14	38.9

Table 2 – Results from Simulation Cases

The charts in Figure 5 show the influence of several variables on slip while other parameters were held constant. Nip load is shown to affect slip in Figure 5(a). Since the nip load also affects mold filling through Equations {5}, {4} and {1} this may not be a practical variable that should be used to control the slip. Also based on the results presented in Figure 5(a) it appears improbable the slip could be forced to vanish through control of the nip load. In Figure 5(b) the effect of the rubber hardness of the backup roller on slip is shown. While the rubber hardness does affect slip it would appear impossible to cause slip to vanish through the selection of this variable. The effect of Poisson's ratio of the backup roller cover is shown in Figure 5(c). Proper selection of Poisson's ratio could drive the slippage to vanish. Low Poisson ratio elastomers can be obtained in the form of open and closed cell foams. In Figure 5(d) the effect of the exit tension after the peel roller is seen on slip. It appears this exit tension could be an effective control variable for causing slip to vanish.

#### **THE NIP-INDUCE-TENSION (NIT)**

The slippage witnessed between the web and the exit of the imprint roller occurs due to the change in web tension and MD web stress that occurred as the web transits through the nip contact zone. This phenomenon has been witnessed in winding webs on winders with impinged nip rollers [5,6]. The change in web tension, in units of load or stress, is known as the Nip-Induced-Tension (NIT). The NIT can be either positive or negative, hence the total web tension after the web exits the nip contact zone ( $T_{out}$ ) can be either larger or smaller than the web tension prior to the nip ( $T_{entry}$ ) in Figure 2:

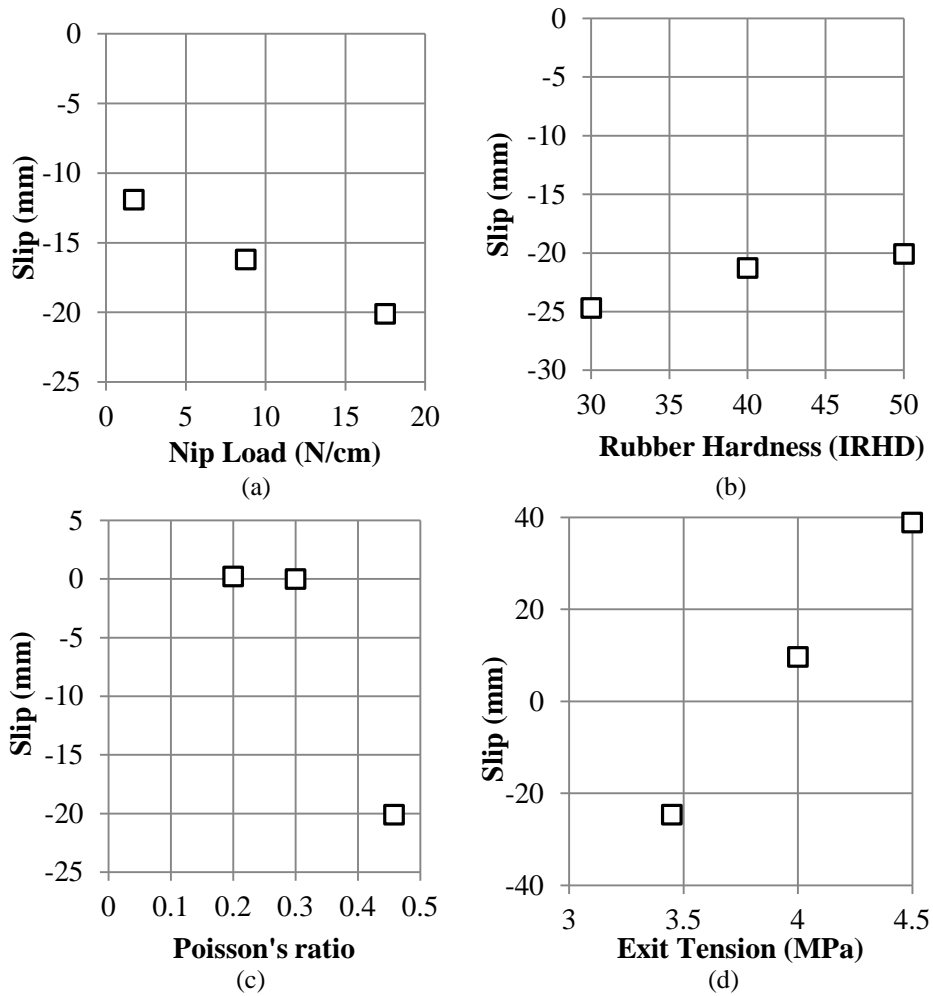


Figure 5 – A study of slippage

$$T_{out} = T_{entry} + NIT \quad \{7\}$$

The NIT and the impact of the NIT on the web tension after the nip contact zone are shown for Case 1 in Figure 6. The NIT is affected by the slippage in the nip contact zone. It has been shown in Figure 3(a) that the width of the contact zone and the pressure variation can be predicted using Equations {5} and {3}, respectively. Thus the shear tractions that could be supported by friction ( $\mu P(x)$ ) shown in Figure 3(c) could also be predicted.

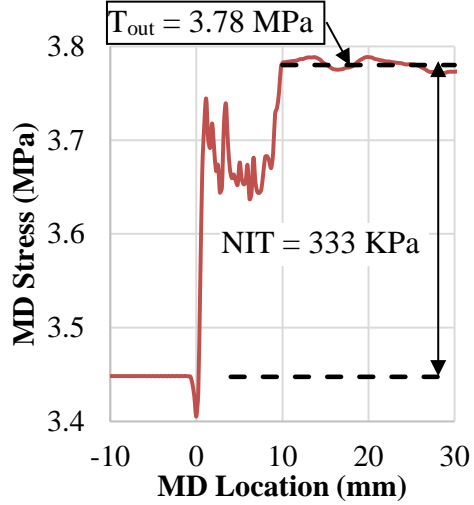


Figure 6 – NIT for Case 1

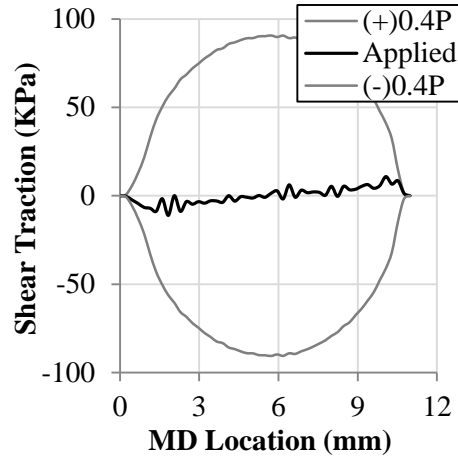


Figure 7 – Web shear on backup roller

The applied shear stress and the frictional shear stresses available to resist slippage between the rubber cover of the backup roller and the web also affect the MD stress and the NIT shown in Figure 7. The applied shear tractions in Figures 3(c) and 7 must be determined using dynamic simulations. The applied shear contact stresses are affected by many variables. Those variables include the web thickness and material properties, the diameters of the backup and imprint rollers, the thickness and properties of the elastomer that covers the backup roller, the nip load and the friction coefficients. The applied shear tractions also impact the MD stresses, the NIT and  $T_{out}$  as shown in Figure 8. In Figure 8, the influence of nip load, the backup roller rubber cover hardness and Poisson's ratio of the cover are shown on the MD stresses while holding other input parameters constant. The NIT and  $T_{out}$  appear sensitive to nip load and Poisson's ratio of the rubber cover but less so to the rubber hardness. Again there are no closed form equations that can predict the tension at the exit ( $T_{out}$ ) of the nip contact zone and thus requiring dynamic simulation to predict slippage.

Elastomer properties can be strain rate and load direction dependent and air entrainment is known to decrease the apparent friction between webs and rollers which could make the NIT and  $T_{out}$  dependent on web velocity, however these complexities are not addressed herein. If the web tension after the exit of the nip contact zone ( $T_{out}$ ) and the tension after the web exits the imprint roller were known ( $T_{exit}$ ) the magnitude and direction of slippage could be predicted with the capstan equation:

$$\begin{aligned}
 \text{If } T_{out} \geq T_{exit} \text{ then slip} &= \frac{R_{impr\ int}}{\mu} \ln \left( \frac{T_{out}}{T_{exit}} \right) \text{ and slip direction } (-) \\
 \text{If } T_{exit} \geq T_{out} \text{ then slip} &= \frac{R_{impr\ int}}{\mu} \ln \left( \frac{T_{out}}{T_{exit}} \right) \text{ and slip direction } (+)
 \end{aligned} \tag{8}$$

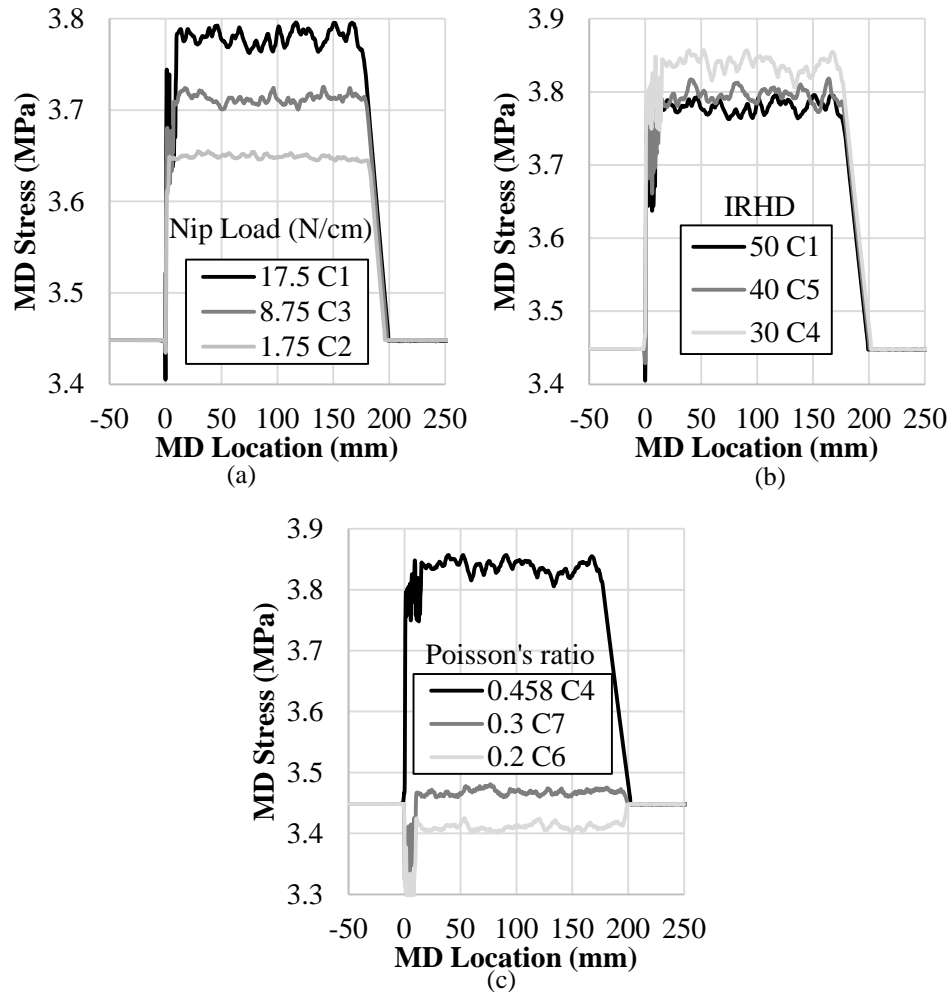


Figure 8 – Effects of nip load (a), rubber hardness (b) and Poisson's ratio of the backup cover (c) on NIT and  $T_{out}$

## CONCLUSIONS

A preliminary study has been conducted to explore the scaling of nanoimprint lithography in R2R manufacturing processes. Equations such as {1} and {4-6} can be used to estimate mold filling in T-NIL and UV-NIL processes. The quality of the nano impressions will be affected by mold filling and also by process chemistry that will allow these imprinted features to cleanly separate from the mold. The preliminary study has shown that zones of slip that are quite large on the nano scale can form in the nip contact zone and in the exit region of the imprint roller. Slip in the nip contact zone is of no consequence for UV-NIL processes and the slip may facilitate mold filling. Large zones of slip near the exit of the imprint roller could abrade or sever nano impressions in UV-NIL processes. Choice of backup cover properties may prevent or reduce the slippage. If the quality of the nano impressed can be assessed on-line it is possible that slippage could

be eliminated through control of the web exit tension from the imprint roller. In T-NIL processes the slippage in the nip contact zone may deter the quality of the thermoplastic nano impressions. Slip on the order of 1 mm was witnessed for the base Case 1 in Figure 3(c) in the nip contact zone, still very large on the nano scale. Slip inside the nip contact zone will be affected minimally by web entering and exiting tension. Minimization of that slip for T-NIL processes will require optimal selection of backup cover properties, design of the backup and imprint rollers and use of dynamic simulations to find optimal designs where the slip is eliminated in the nip contact zone.

In T-NIL processes the viscosity of the thermoplastic will be changing after the impressions are formed and begin cooling. In UV-NIL processes the viscosity of the resin will be low at the entry of the nip but the elasticity of the resin will increase as the resin is cured prior to exiting the imprint roll. These complexities have not been addressed in the dynamic simulations presented herein. Multiphysics simulations would be required to study the combined effects of fluids becoming elastic in conjunction with the surface/contact mechanics of a rolling nip.

## ACKNOWLEDGMENTS

Portions of this work were supported by the National Science Foundation under Grant 1635636 and by the Web Handling Research Center of Oklahoma State University. Any opinions, findings, and conclusions or recommendations expressed in this material are those of the author(s) and do not necessarily reflect the view of the National Science Foundation.

## REFERENCES

1. Dumond, J. J., and Low, H. Y., "Recent Developments and Design Challenges in Continuous Roller Micro- and Nanoimprinting," J. Vac. Sci. Technol. B, Vol. 30, No. 1, Jan/Feb 2012.
2. Ahn, S. H., and Guo, L. J., "Large-Area Roll-to-Roll and Roll-to-Plate Nanoimprint Lithography: A Step toward High-Throughput Application of Continuous Nanoimprinting," ACS NANO, Vol. 3, No. 8, 2009.
3. Ahn, S. H., and Guo, L. J., "High-Speed Roll-to-Roll Nanoimprint Lithography on Flexible Plastic Substrates," Adv. Mater., Vol. 20, No. 11, 2008, pp. 2044-2049.
4. Cole, K., "Modeling of Nip Pressures and Web Feed Rates in Rubber Covered Nip Rollers," Proceedings of the 12<sup>th</sup> International Conference on Web Handling, Web Handling Research Center, Oklahoma State University, Stillwater, Oklahoma, June 2-5, 2013.
5. Ren, Y., Kandadai, B., and Good, J.K., "Center Winding versus Surface Winding: The Effect of Winder Type and Web Material Properties on Wound Roll Stresses," Transactions of the 15th Fundamental Research Symposium, Cambridge, England, September, 2013.
6. Ren, Y., Kandadai, B., and Good, J.K., "The Effect of Winder Type and Web Material Properties on Wound-On-Tension," Proceedings of the Twelfth International Conference on Web Handling, Web Handling Research Center, Stillwater, Oklahoma, June 2-5, 2013.
7. Blevins, R.D., Applied Fluid Dynamics Handbook, Krieger Publishing Company, Malabar, Florida, 1992, pp. 501-503.

8. Good, J. K., "Modeling Rubber Covered Rollers in Web Lines," Proceedings of the Sixth International Conference on Web Handling, Web Handling Research Center, Stillwater, Oklahoma, June 10-13, 2001, pp. 159-178.
9. ASTM D575, "Standard Test Methods for Rubber Properties in Compression," Annual Book of ASTM Standards, 100 Barr Harbor Dr., West Conshohocken, PA, USA.
10. Johnson, K.L., Contact Mechanics, Cambridge University Press, 1989, pp. 139-140.